Int. J. Electrochem. Sci., 17 **(2022)** Article Number: 220225, doi: 10.20964/2022.02.32

International Journal of
ELECTROCHEMICAL
SCIENCE
www.electrochemsci.org

Nanofiber-based $Sm_{0.5}Sr_{0.5}Co_{0.2}Fe_{0.8}O_{3-\delta}$ of N-doped graphene modification for bifunctional oxygen electrocatalyst in alkaline medium

Yuwei Wang, Ying Yue, Tao Cong, Liquan Fan, Xinyu Su, Xingmei Liu, WeiChao Zhang, Yufeng Li, Xijun Liu*

College of Materials Science and Engineering, Heilongjiang Provincial Key Laboratory of Polymeric Composite Materials, Qiqihar University, No.42, Wenhua Street, Qiqihar 161006, PR China
*E-mail: Liquan_Fan@163.com

Received: 27 October 2021 / *Accepted:* 1 December 2021 / *Published:* 5 January 2022

The development of electrocatalysts with excellent OER and ORR performance is a significant challenge for the commercialization of metal-air batteries. We report $Sm_{0.5}Sr_{0.5}Co_{0.2}Fe_{0.8}O_{3-\delta}$ (SSCF28) nanofibers modified by 3D nitrogen-doped graphene (3DNG) composite catalysts with different mass ratios of SSCF28:3DNG. In 0.1 M KOH electrolyte, SSCF28/3DNG with the optimal mass ratio (1:1) demonstrates the best oxygen electrocatalysis performance. The synergistic effect between SSCF and 3DNG benefits the electrocatalytic activities of OER and ORR.

Keywords: $Sm_{0.5}Sr_{0.5}Co_{0.2}Fe_{0.8}O_{3-\delta}$; N-doped graphene; Nanofibers; OER; ORR

1. INTRODUCTION

The energy problem sparks the focus of scientists all over the world. With the aggravation of pollution and exhaustion of petroleum resources, it is urgent to find new clean energy to replace the traditional fossil energy. A metal-air battery is an effective electrochemical conversion device that can solve energy problems. However, the technical hurdles must be cleared before metal-air batteries can be commercialized. The performance of metal-air cells is mainly related to two critical electrochemical reaction steps: oxygen reduction reaction (ORR) and oxygen precipitation reaction (OER) [1-2]. As a sort of noble metal substitute, perovskites have attracted much attention in electrocatalysis because of their low price, unique crystal structure, and flexible regulation. Da et al. [3] reported that $Sr_{0.95}Co_{0.8}Fe_{0.2}O_{3-\delta}$ shows good OER performance. $PrBa_{0.5}Sr_{0.5}Co_{1.5}Fe_{0.5}O_{5+\delta}$ (PBSCF) was found to have good OER performance. In 0.1 M KOH, the initial OER potential of PBSCF was 1.53V, and the

overpotential of PBSCF was 359 mV at 10 mA cm^{-2} [4]. $La_{1.5}Sr_{0.5}NiMn_{0.5}Ru_{0.5}O_6$ (LSNMR) exhibits excellent bi-functional electrocatalytic activities and good stability[5]. The introduction of metal elements with high catalytic activity in the B-site metal elements into perovskite oxides will affect the oxygen vacancy concentration and electronic structure of electrocatalysts, which is conducive to improving OER/ORR performance. In addition, carbon materials can play a vital role in improving the electrocatalysis of perovskites. Stoerzinger et al. [6] demonstrated that $La_{(1-x)}Sr_xMnO_3$ (LSMO) perovskite with the lower valence band center close to the Fermi level has the better ORR activity.

Perovskite materials perform well in electrocatalysis, but their low electrical conductivity at room temperature limits the intrinsic electrocatalytic activity. People usually add carbon materials as the conductive phase in testing process to solve such problems [7,8]. The introduction of functionalized acetylene black (AB_f) into $Ba_{0.5}Sr_{0.5}Co_{0.8}Fe_{0.2}O_{3-\delta}$ or $(Pr_{0.5}Ba_{0.5})CoO_{3-\delta}$ (PBCO) results in the significant enhancement of OER activity of the perovskite oxides[9]. The ORR performance of $La_{0.6}Ca_{0.4}CoO_3$ - Vulcan carbon (LCCO-C) composite catalyst was significantly higher than that of LCCO [10]. In this study, we prepared $Sm_{0.5}Sr_{0.5}Co_{0.2}Fe_{0.8}O_{3-\delta}$ (SSCF28) nanofibers, and designed SSCF28/3DNG composite catalysts by the introduction of 3DNG, and assessed the probability of SSCF28/3DNG as bi-functional catalytic activity in terms of ORR and OER.

2. EXPERIMENTAL SECTION

2.1. Preparation of SSCF/3DNG composite catalysts

Three-dimensional nitrogen-doped graphene (3DNG) was prepared by the hydrothermal method [11]. The conductivity of graphene can be further improved, and more active sites can be introduced by doping N element. $Sm_{0.5}Sr_{0.5}Co_{0.2}Fe_{0.8}O_{3-\delta}$ (SSCF28) nanofibers were prepared by electro-spinning. The stoichiometric amounts of $Sm(NO_3)_3 \cdot 6H_2O$, $Sr(NO_3)_2$, $Co(NO_3)_2 \cdot 6H_2O$ and $Fe(NO_3)_3 \cdot 9H_2O$ with molar ratios of 0.5:0.5:0.2:0.8 were added into N,N-dimethylformamide (DMF) solvent under stirring to get a clear solution . Then the appropriate amount of polyvinylpyrrolidone (PVP) was added into the above solution to form the electrospinning solution. The as-electrospun SSCF28 nanofibers were calcined at 800 °C in air for 2 h to obtain SSCF28 nanofibers.

SSCF28 nanofibers and 3DNG were uniformly mixed by sonication to prepare SSCF28/3DNG composite catalysts with different mass ratios (SSCF28: DNG=1:2, 1:1, 2:1).

2.2 Characterization and electrochemical test

The microstructure and phase formation of SSCF28, 3DNG, and SSCF28/3DNG were examined by scanning electron microscopy (SEM, S-3400, Japan) and X-ray diffraction (XRD, BRUKER-AXS D8, German) using Cu-Ka radiation, respectively. The surface morphology and elemental distribution of SSCF28/3DNG were analyzed by transmission electron microscopy (TEM, HITACHI H-7650, Japan) and EDS elemental mapping in TEM. Carbon-coated copper grids were used as the sample holders.

Standard three-electrode system was used for electrochemical measurement. The glassy carbon electrode (GCE) was used as the working electrode, the Ag/AgCl electrode as the reference electrode, and the platinum wire as the auxiliary electrode. The electrolyte used was 0.1 M KOH solution.

Electrochemical impedance spectra were measured by using an electrochemical workstation (CHI 760E, China). ORR/OER electrochemical tests were performed on a rotating ring disk electrode device (RRDE, ALS Co., Ltd.). The GCE midified by SSCF28/3DNG was used as the working electrode (diameter: 4 mm), Ag/AgCl as the reference electrode, and platinum wire as the counter electrode. During the OER/ORR test, the rotating rate of the electrode was 1600 rpm, and the scan rate was 5 mV/s. And the electron transfer number (n) generated in the ORR process was calculated according to the literature [12].

3. RESULTS AND DISCUSSION

Fig. 1 (a) and (b) show the electrochemical impedance spectra of SSCF28/3DNG and 3DNG at 1.664 V, respectively. The resistance of SSCF28/3DNG (1:1) is 70 Ω, which is less than the single SSCF28, 3DNG, and the other composites. Graphene is a two-dimensional monatomic layer carbon material with excellent electrical conductivity. However, most graphene prepared is multilayer, and the intense attraction between graphene sheets limits its electrical conductivity. For 3DNG, the graphene sheets are connected to form 3D skeleton structure to obtain excellent electrical conductivity, similar to that of monolayer graphene. Moreover, the conductivity of 3DNG is further improved due to the doping of nitrogen. The introduction of 3DNG has obviously enhanced the electronic conductivity of SSCF28, and SSCF28/3DNG (1:1) has the best electronic conductivity.

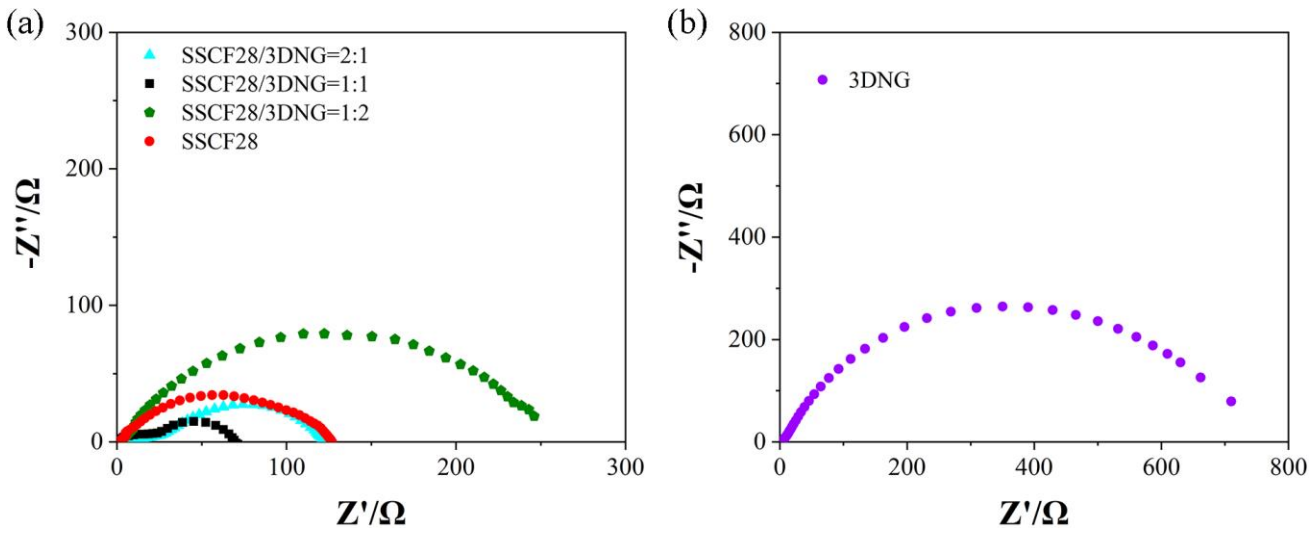

Figure 1. Electrochemical impedance spectra of (a) SSCF28/3DNG and (b) 3DNG at 1.664 V (vs. RHE)

As depicted in Fig. 2 (a), SSCF28 shows a well-connected nanofiber structure. Fig. 2(b) is a typical SEM image of 3DNG. 3DNG presents a 3D spatial structure composed of layers of graphite,

which increases its specific surface area and has more reactive sites. As shown in Fig. 2(c) and (d), SEM and TEM test results show that SSCF28 nanofibers are evenly inserted in the interlayer of 3DNG. Fig. 2(d_1)-(d_7) is the EDS mapping images of Fig. 2(d), Sm, Sr, Co, Fe, O, C and N elements are evenly distributed, which further indicates that SSCF28 nanofibers are evenly inserted between the 3DNG interlayers.

Fig. 3 illustrates the XRD spectra of SSCF28, 3DNG, and SSCF28/3DNG (1:1). The diffraction peaks of SSCF28 are sharp and intense, indicating SSCF28 is highly crystalline. The XRD pattern of 3DNG shows broad, amorphous features and no peaks indicative of crystalline phases. The pattern for SSCF28/3DNG has several peaks that can be well-indexed to (101), (121), (220), (202), (123), and (242) of SSCF28. The weak carbon peaks appear in SSCF28/3DNG, owning to the low loading content of 3DNG. SSCF28/3DNG were prepared by ultrasonic mixing. 3DNG did not affect the perovskite phase SSCF28 in SSCF28/3DNG. The existence of the C element can also be proved by EDS analysis. As shown in Fig. 3 (d_6), the carbon element exists and is evenly distributed in SSCF28/3DNG composite catalyst.

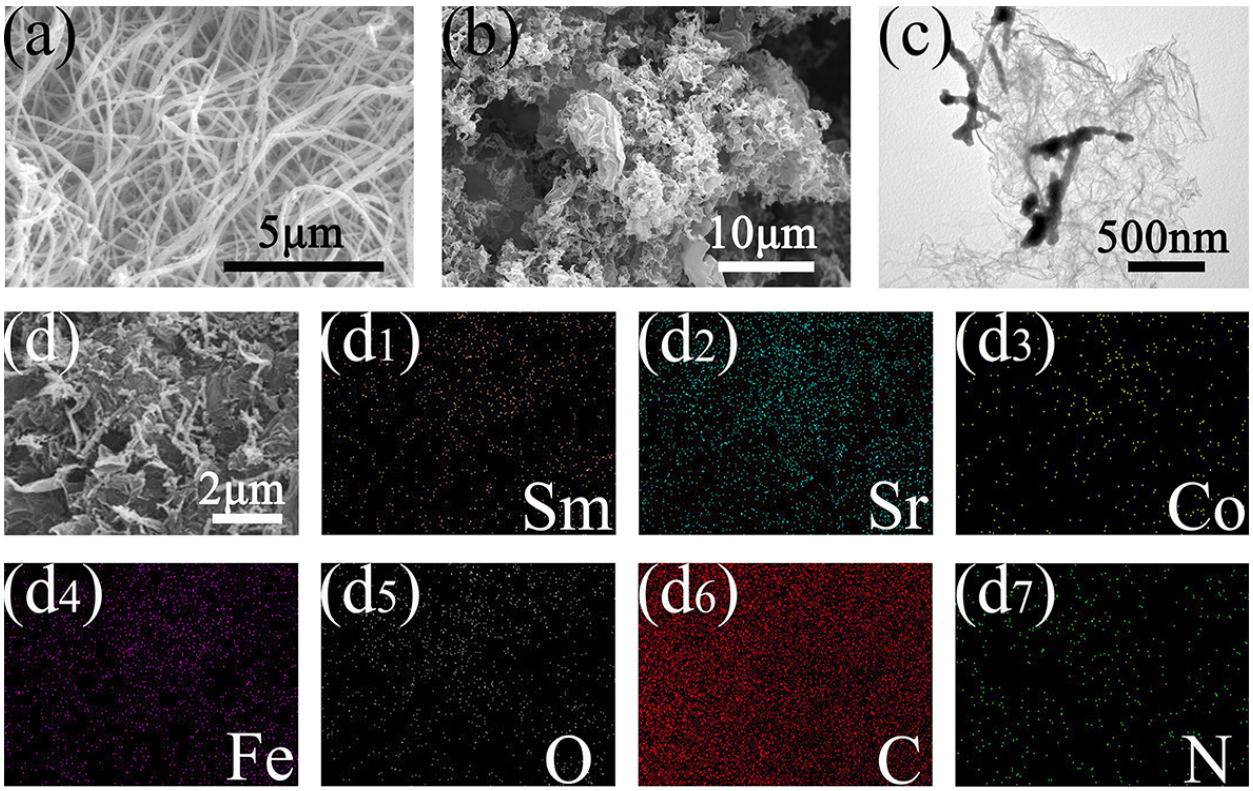

Figure 2. SEM images of (a) SSCF28 and (b) 3DNG . (c) TEM image of SSCF28/3DNG. (d) EDS element mapping SSCF28/3DNG.

To explore whether the introduction of 3DNG can enhance the OER performance of SSCF28 nanofiber perovskite, the OER performance of SSCF28/3DNG composite catalyst with different mass ratios was examined. Fig. 4 (a) and (b) show the polarization curve and Tafel slope of SSCF28/3DNG composite catalyst, respectively. As shown in Fig. 4 (a), the potential of SSCF28/3DNG (1:1) reaches

10 mA cm^{-2}, which is better than the other composite catalysts. Accordingly, the tafel slope value of SSCF28/3DNG (1:1) is the lowest value of only 81 mV dec^{-1}.

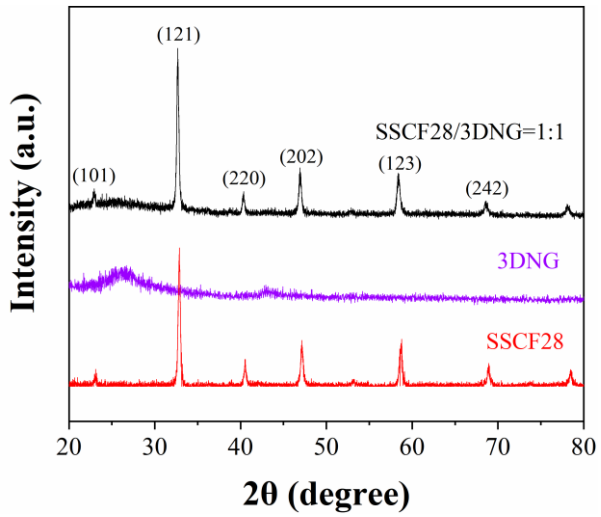

Figure 3. XRD spectra of SSCF28, 3DNG and SSCF28/3DNG (1:1)

The results indicate that SSCF28/3DNG (1:1) has the best OER catalytic performance, greater than comparable reported value in literature [12]. The introduction of 3DNG successfully improves the OER performance of SSCF28 nanofiber perovskite. When the mass ratio of SSCF28 to 3DNG is 1:1, the OER performance is the strongest. Due to its unique crystal structure, SSCF28 has many oxygen vacancies on the perovskite surface, which is conducive to the evolution reaction of oxygen. Moreover, the unique one-dimensional nanofiber structure of SSCF28 dramatically increases the contact area between SSCF28 and oxygen and electrolyte. All these factors are favorable for the OER reaction. However, the resistance of perovskite materials is too high under the room temperature condition, resulting in the slow process of electron transfer to the active site and reaction, which seriously affects the reaction rate of OER. Due to its 3D honeycomb spatial structure, 3DNG overcomes the intense attraction between graphene sheets and shows a conductivity close to monolayer graphene. Moreover, due to the doping of nitrogen, the conductivity of graphene is further improved. Through ultrasonic mixing, SSCF28 nanofibers are evenly inserted into the 3DNG layers to maximize the electrical conductivity of 3DNG and successfully release the inherent electrocatalytic activity of SSCF28. The electron transport takes happen from 3DNG to oxygen and SSCF28, resulting in the enhancement of the electrocatalytic activity [14]. In addition, the 3D porous structure of SSCF28/3DNG can provide more reactive sites and oxygen transport channels, which makes the catalyst show better OER performance.

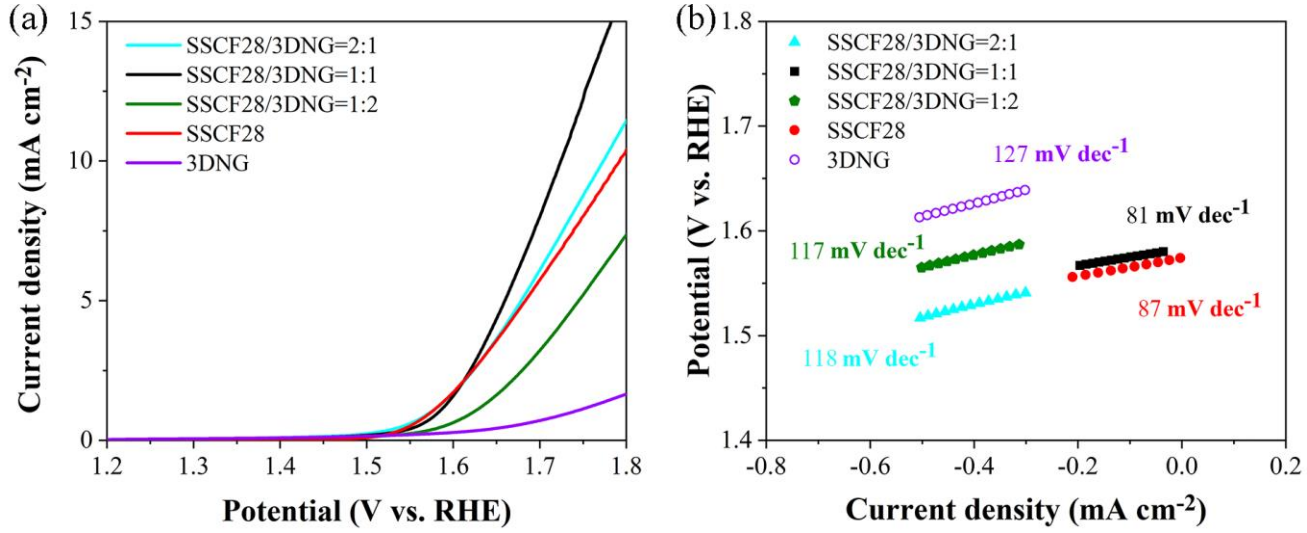

Figure 4. OER activity of SSCF28/3DNG: (a) Polarization curve, (b) Tafel plots obtained from the polarization curves in OER process.

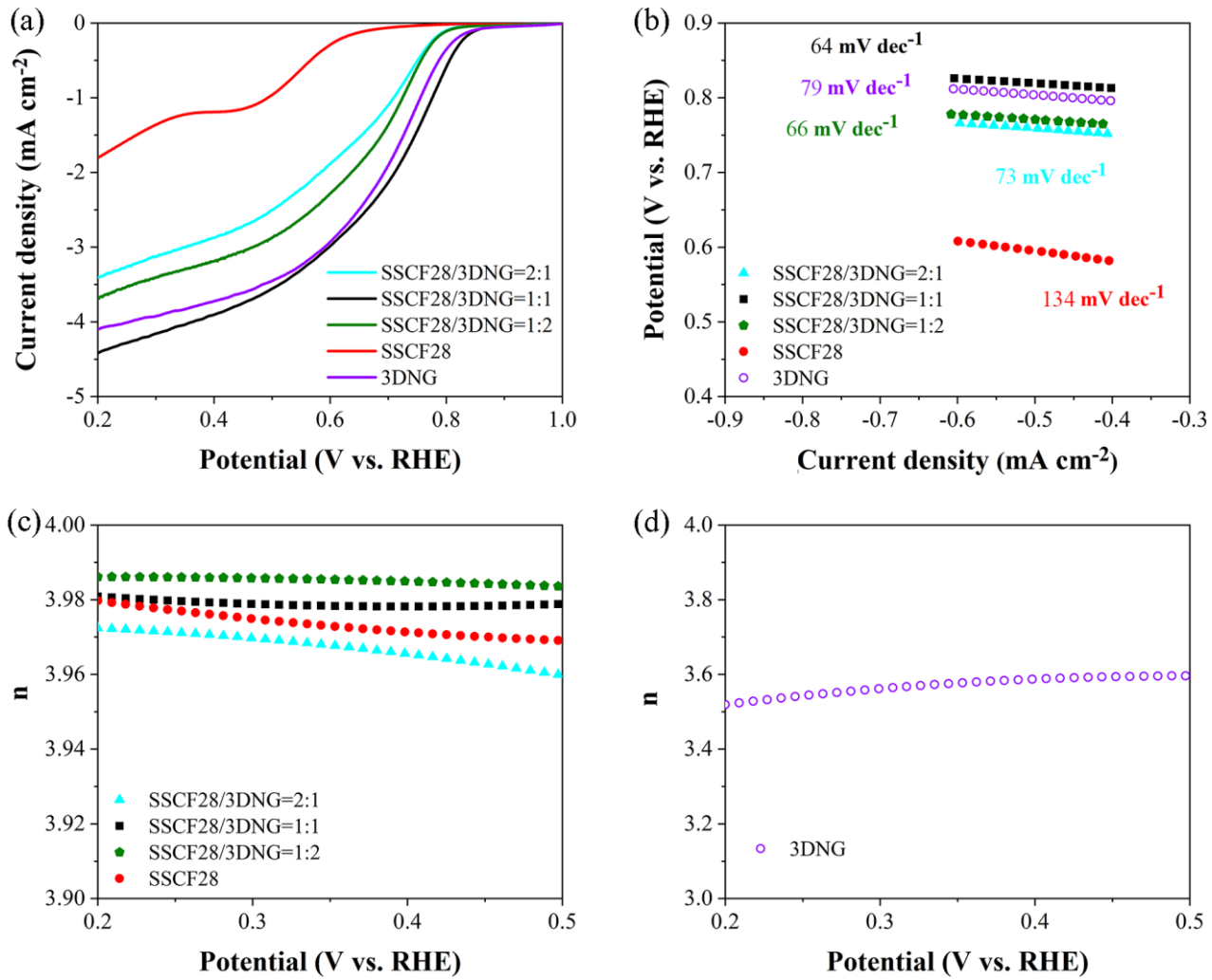

Figure 5. ORR activity of SSCF28/3DNG: (a) Polarization curve; (b) Tafel plots obtained from the polarization curves in ORR process; (c) and (d) The electron-transfer numbers

In order to explore whether the introduction of 3DNG can enhance the ORR performance of SSCF28 nanofiber perovskite, the ORR performance of SSCF28/3DNG composite catalyst with different mass ratios was tested. Fig. 5(a) shows the polarization curve of SSCF28/3DNG. SSCF28/3DNG (1:1) has a current density of 4.42 mA cm^{-2} and a half-wave potential of 0.69 V at 0.2 V, showing the best ORR performance. Fig. 5 (b) shows the Tafel curve of SSCF28/3DNG composite catalyst. The Tafel slope of SSCF28/3DNG (1:1) exhibits the lowest value of only 64 mV dec^{-1}. As shown in Fig. 5(c) and (d), both SSCF28 and SSCF28/3DNG composite catalysts show high n values, which are close to 4, while 3DNG has a lower n value. The ORR test results can prove that the introduction of 3DNG successfully improves the ORR performance of SSCF28 nanofiber perovskite. In summery, when the mass ratio of SSCF28 to 3DNG is 1:1, the ORR performance is the strongest. SSCF28 nanofiber is a perovskite oxide, and its surface contains a large number of oxygen vacancies. The existence of oxygen vacancies is conducive to the adsorption and desorption of oxygen-containing species, which is beneficial to the ORR reaction. The doping of N atoms not only further improves the conductivity of graphene, but also provides more active sites for electrocatalytic reactions. This is because the electronegativity of N is greater than that of C, which is conducive to the ORR reaction. , the 3D porous structure of SSCF28/3DNG favors the oxygen transport, which is also crucial for obtaining excellent ORR catalytic activity.

The SSCF28/3DNG composite catalyst has excellent OER and ORR performance simultaneously, and benefits from spillover effect between perovskite and carbon in addition to enhanced electrical conductivity [14,15]. As shown in Figure 6, in the OER process, perovskite oxide SSCF plays a leading role. During the reaction process, excess oxygen is spilled onto the 3DNG surface, releasing more active sites on the SSCF28 surface. The spillover effect is not only reflected in the OER process, but also the ORR process. In the ORR reaction dominated by 3DNG, excess OH- spills from the carbon surface to the SSCF surface, releasing more active sites on the 3DNG surface.

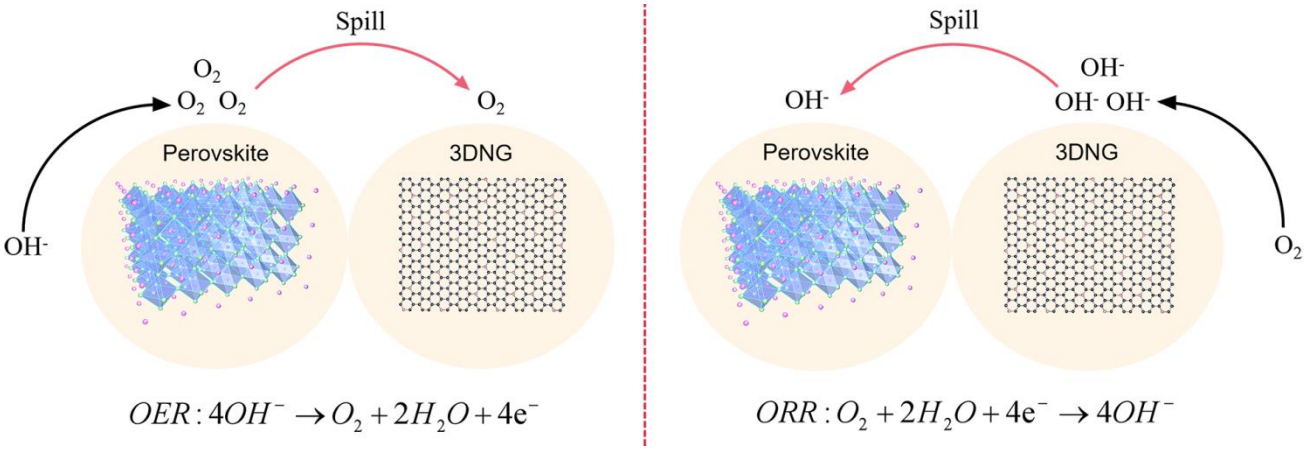

Figure 6. Diagram of spillover effects

4. CONCLUSIONS

3DNG was prepared by the hydrothermal method. The prepared 3DNG has a large specific surface area, excellent electrical conductivity, and more active sites for electrocatalytic reaction. The addition of 3DNG can effectively improve the electronic conductivity of SSCF28 nanofiber perovskite, making SSCF28/3DNG composite catalyst show good OER/ORR performance. SSCF28/3DNG (1:1) has the best electrocatalytic performance. This kind of bi-functional perovskite-carbon electrocatalyst with excellent performance has a potential application prospect in the field of metal-air batteries.

ACKNOWLEDGMENTS
The authors want to acknowledge the Natural Science Foundation of Heilongjiang Province, China (No. LH2019E092) and the Fundamental Research Funds in Heilongjiang Provincial Universities (No. 135309347).

References

1. C. Xia, C.Y. Kwok, L.F. Nazar, *Science*, 361 (2018) 777.
2. W. Sun, F. Wang, B. Zhang, M. Zhang, V. Küpers, X. Ji, C. Theile, P. Bieker, K. Xu, C. Wang, M. Winter, *Science*, 371 (2021) 46.
3. Y. Da, L. Zeng, C. Wang, C. Gong, L. Cui, *Electrochim. Acta*, 300 (2019) 85.
4. H. Yu, F. Chu, X. Zhou, J. Ji, Y. Liu, Y. Bu, Y. Kong, Y. Tao, Y. Li, Y. Qin, *Chem. Commun.*, 55 (2019) 2445.
5. M. Retuerto, F. Calle-Vallejo, L. Pascual, G. Lumbeeck, M.T. Fernandez-Diaz, M. Croft, J. Gopalakrishnan, M.A. Pena, J. Hadermann, M. Greenblatt, Sergio. Rojas, *ACS Appl. Mater. Interfaces*, 11 (2019) 21454.
6. K.A. Stoerzinger, W.T. Hong, X.R. Wang, R.R. Rao, S.B. Subramanyam, C. Li, Ariando, T. Venkatesan, Q. Liu, E.J. Crumlin, K.K. Varanasi, and Y. Shao-Horn, *Chem. Mater.* 23 (2017) 9990.
7. S. Velraj, J.H. Zhu, *J. Power Sources*, 227 (2013) 48.
8. Z. Wang, Y. You, J. Yuan, Y. Yin, Y. Li, S. Xin, and D. Zhang, *ACS Appl. Mater. Interfaces*, 8 (2016) 6520.
9. R. Mohamed, X. Cheng, E. Fabbri, P. Levecque, R. Kötz, O. Conrad, and T.J. Schmidt, *J. Electrochem. Soc.*, 162 (2015) F579.
10. X. Li, W. Qu, J. Zhang, H. Wang, *J. Electrochem. Soc.*, 158 (2011) A597.
11. Y. Qin, J. Yuan, J. Li, D. Chen , Y. Kong , F. Chu , Y. Tao , and M. Liu, *Adv. Mater.*, 27 (2015) 5171.
12. C. Wu, H. Cheng, K. Xu, L. Xing, S. Liu, Y. Gong, L. Gu, L. Zhang, *J. Mater. Chem. A*, 4 (2016) 11775.
13. Y. Zhang, Y. Guo, T. Liu, F. Feng, C. Wang, H. Hu, M. Wu, M. Ni, Z.Shao, *Front. Chem.*, 7 (2019) 524.
14. Y. Bu, G. Nam, S. Kim, K. Choi, Q. Zhong, J.H. Lee, Y. Qin, J. Cho, G. Kim, *Small*, 14 (2018) 1802767.
15. Y. Zhu, W. Zhou, Z. Shao, *Small*, 13 (2017) 1603793.